Breakdown of the linear acousto-optic interaction regime in phoxonic cavities

Evangelos Almpanis,[1] Nikolaos Papanikolaou,[1,*] and Nikolaos Stefanou[2]

[1]*Institute of Nanoscience and Nanotechnology, NCSR "Demokritos,"GR-153 10 Athens, Greece*

[2]*Department of Solid State Physics, University of Athens, Panepistimioupolis, GR-157 84 Athens, Greece*

[*]*N.Papanikolaou@imel.demokritos.gr*

Abstract: The limits of validity of the linear photoelastic model are investigated in a one-dimensional dual photonic-phononic cavity, formed by alternating layers of a chalcogenide glass and a polymer homogeneous and isotropic material, which supports both optical and acoustic resonant modes localized in the same region. It is shown that the linear-response regime breaks down when either the acoustic excitation increases or the first-order acousto-optic interaction coupling element vanishes by symmetry, giving rise to the manifestation of multiphonon absorption and emission processes by a photon. Our results provide a consistent interpretation of different aspects of the underlying physics relating to nonlinear acousto-optic interactions that can occur in such cavities.

OCIS codes: (160.1050) Acousto-optical materials; (190.5890) Scattering, stimulated; (310.4165) Multilayer design.

References and links

1. A. Yariv and P. Yeh, *Optical Waves in Crystals* (John Wiley and Sons, 2003).
2. J. N. Winn, S. Fan, J. D. Joannopoulos, and E. P. Ippen, "Interband transitions in photonic crystals," Phys. Rev. B **59**(3), 1551 (1999).
3. H. Ma, S. Qu, and Z. Xu, "Photonic crystals based on acousto-optic effects," J. Appl. Phys. **103**(10), 104904 (2008).
4. J. R. Zurita-Sánchez, P. Halevi, and J. C. Cervantes-González, "Reflection and transmission of a wave incident on a slab with a time-periodic dielectric function $\varepsilon(t)$," Phys. Rev. A **79**(5), 053821 (2009).
5. J. C. Hsu, C. H. Lin, Y. C. Ku, and T. R. Lin, "Photonic band gaps induced by submicron acoustic plate waves in dielectric slab waveguides," Opt. Lett. **38**(20), 4050–4053 (2013).
6. S. Krishnamurthy and P. V. Santos, "High-contrast optical modulation by surface acoustic waves," Appl. Phys. Lett. **83**(13), 2548–2550 (2003).
7. X. S. Qian, J. P. Li, M. Lu, Y. Lu, and Y. Chen, "Acousto-optic interaction in photonic crystals with defects," J. Appl. Phys. **106**(4), 043107 (2009).
8. N. Courjal, S. Benchabane, J. Dahdah, G. Ulliac, Y. Gruson, and V. Laude, "Acousto-optically tunable lithium niobate photonic crystal," Appl. Phys. Lett. **96**(13), 131103 (2010).
9. C. Thomsen, H. T. Grahn, H. J. Maris, and J. Tauc, "Surface generation and detection of phonons by picosecond light pulses," Phys. Rev. B **34**(6), 4129 (1986).
10. N. D. Lanzillotti-Kimura, A. Fainstein, A. Huynh, B. Perrin, B. Jusserand, A. Miard, and A. Lemaître, "Coherent generation of acoustic phonons in an optical microcavity," Phys. Rev. Lett. **99**(21), 217405 (2007).
11. J. -F. Robillard, A. Devos, I. Roch-Jeune, and P. A. Mante, "Collective acoustic modes in various two-dimensional crystals by ultrafast acoustics: Theory and experiment," Phys. Rev. B **78**(6), 064302 (2008).
12. T. Berstermann, C. Brüggemann, M. Bombeck, A. V. Akimov, D. R. Yakovlev, C. Kruse, D. Hommel, and M. Bayer, "Optical bandpass switching by modulating a microcavity using ultrafast acoustics," Phys. Rev. B **81**(8), 085316 (2010).

#222544 - $15.00 USD Received 4 Sep 2014; revised 28 Oct 2014; accepted 2 Nov 2014; published 15 Dec 2014

13. P. M. Walker, J. S. Sharp, A. V. Akimov, and A. J. Kent, "Coherent elastic waves in a one-dimensional polymer hypersonic crystal," Appl. Phys. Lett. **97**(7), 073106 (2010).
14. A. Fainstein, N. D. Lanzillotti-Kimura, B. Jusserand, and B. Perrin, "Strong optical-mechanical coupling in a vertical GaAs/AlAs microcavity for subterahertz phonons and near-infrared light," Phys. Rev. Lett. **110**(3), 037403 (2013).
15. D. J. Farmer, A. V. Akimov, N. A. Gippius, J. Bailey, J. S. Sharp, and A. J. Kent, "High-frequency acousto-optic effects in Bragg reflectors," Opt. Express **22**(12), 15218–15231 (2014).
16. M. Trigo, A. Bruchhausen, A. Fainstein, B. Jusserand, and V. Thierry-Mieg, "Confinement of acoustical vibrations in a semiconductor planar phonon cavity," Phys. Rev. Lett. **89**(22), 227402 (2002).
17. J. Groenen, F. Poinsotte, A. Zwick, C. M. Sotomayor Torres, M. Prunnila, and J. Ahopelto, "Inelastic light scattering by longitudinal acoustic phonons in thin silicon layers: From membranes to silicon-on-insulator structures," Phys. Rev. B **77**(4), 045420 (2008).
18. N. Gomopoulos, D. Maschke, C. Y. Koh, E. L. Thomas, W. Tremel, H.-J. Butt, and G. Fytas, "One-dimensional hypersonic phononic crystals," Nano Lett. **10**(3), 980–984 (2010).
19. T. Gorishnyy, M. Maldovan, C. Ullal, and E. L. Thomas, "Sound ideas," Phys. World **18**(12), 24–29 (2005).
20. I. E. Psarobas, N. Papanikolaou, N. Stefanou, B. Djafari-Rouhani, B. Bonello, and V. Laude, "Enhanced acousto-optic interactions in a one-dimensional phoxonic cavity," Phys. Rev. B **82**(17), 174303, (2010).
21. N. Papanikolaou, I. E. Psarobas, N. Stefanou, B. Djafari-Rouhani, B. Bonello, and V. Laude, "Light modulation in phoxonic nanocavities," Microel. Eng. **90**, 155–158 (2012).
22. E. Almpanis, N. Papanikolaou, G. Gantzounis, and N. Stefanou, "Tuning the spontaneous light emission in phoxonic cavities," J. Opt. Soc. Am. B **29**(9), 2567–2574 (2012).
23. J. Manzanares-Martinez, D. Moctezuma-Enriquez, Y. J. Rodriguez-Viveros, B. Manzanares-Martinez, and P. Castro-Garay, "Non-perpendicular hypersonic and optical stop-bands in porous silicon multilayers," Appl. Phys. Lett. **101**(26), 261902 (2012).
24. M. Maldovan and E. L. Thomas, "Simultaneous complete elastic and electromagnetic band gaps in periodic structures," Appl. Phys. B: Lasers and Optics **83**(4), 595–600 (2006).
25. M. Maldovan and E. L. Thomas, "Simultaneous localization of photons and phonons in two-dimensional periodic structures," Appl. Phys. Lett. **88**(25), 251907 (2006).
26. S. Sadat-Saleh, S. Benchabane, F. I. Baida, M. P. Bernal, and V. Laude, "Tailoring simultaneous photonic and phononic band gaps," J. Appl. Phys. **106**(7), 074912 (2009).
27. D. Bria, M. B. Assouar, M. Oudich, Y. Pennec, J. Vasseur, and B. Djafari-Rouhani, "Opening of simultaneous photonic and phononic band gap in two-dimensional square lattice periodic structure," J. Appl. Phys. **109**(1), 014507 (2011).
28. T. X. Ma, Y. S. Wang, and C. Zhang, "Investigation of dual photonic and phononic bandgaps in two-dimensional phoxonic crystals with veins," Opt. Commun. **312**, 68–72 (2014).
29. Y. El Hassouani, C. Li, Y. Pennec, E. H. El Boudouti, H. Larabi, A. Akjouj, O. B. Matar, V. Laude, N. Papanikolaou, A. Martinez, and B. Djafari-Rouhani, "Dual phononic and photonic band gaps in a periodic array of pillars deposited on a thin plate," Phys. Rev. B **82**(15), 155405 (2010).
30. S. Mohammadi, A. A. Eftekhar, A. Khelif, and A. Adibi, "Simultaneous two-dimensional phononic and photonic band gaps in opto-mechanical crystal slabs," Opt. Express **18**(9), 9164–9172 (2010).
31. Y. Pennec, B. Djafari-Rouhani, E. H. El Boudouti, C. Li, Y. El Hassouani, J. O. Vasseur, N. Papanikolaou, S. Benchabane, V. Laude, and A. Martinez, "Simultaneous existence of phononic and photonic band gaps in periodic crystal slabs," Opt. Express **18**(13), 14301–14310 (2010).
32. N. Papanikolaou, I. Psarobas, and N. Stefanou, "Absolute spectral gaps for infrared light and hypersound in three-dimensional metallodielectric phoxonic crystals," Appl. Phys. Lett. **96**(23), 231917 (2010).
33. T. X. Ma, Y. S. Wang, Y. F. Wang, and X. X. Su, "Three-dimensional dielectric phoxonic crystals with network topology," Opt. Express **21**(3), 2727–2732 (2013).
34. V. Laude, J. C. Beugnot, S. Benchabane, Y. Pennec, B. Djafari-Rouhani, N. Papanikolaou, J. M. Escalante, and A. Martinez, "Simultaneous guidance of slow photons and slow acoustic phonons in silicon phoxonic crystal slabs," Opt. Express **19**(10), 9690–9698 (2011).
35. Y. Pennec, B. Djafari-Rouhani, C. Li, J. M. Escalante, A. Martinez, S. Benchabane, V. Laude, and N. Papanikolaou, "Band gaps and cavity modes in dual phononic and photonic strip waveguides," AIP Advances **1**(4), 041901 (2011).
36. J. M. Escalante, A. Martínez, and V. Laude, "Design of single-mode waveguides for enhanced light-sound interaction in honeycomb-lattice silicon slabs," J. Appl. Phys. **115**(6), 064302 (2014).
37. T. X. Ma, Y. S. Wang, C. Zhang, and X. X. Su, "Simultaneous guiding of slow elastic and light waves in three-dimensional topology-type phoxonic crystals with a line defect," J. Opt. **16**(8), 085002 (2014).
38. J. Gomis-Bresco, D. Navarro-Urrios, M. Oudich, S. El-Jallal, A. Griol, D. Puerto, E. Chavez, Y. Pennec, B. Djafari-Rouhani, F. Alzina, A. Martínez, and C. M. Sotomayor Torres, "A one-dimensional optomechanical crystal with a complete phononic band gap," Nat. Commun. **5**, 4452 (2014).
39. F. L. Hsiao, C. Y. Hsieh, H. Y. Hsieh, and C. C. Chiu, "High-efficiency acousto-optical interaction in phoxonic nanobeam waveguide," Appl. Phys. Lett. **100**(17), 171103 (2012).

#222544 - $15.00 USD Received 4 Sep 2014; revised 28 Oct 2014; accepted 2 Nov 2014; published 15 Dec 2014

40. Q. Rolland, M. Oudich, S. El-Jallal, S. Dupont, Y. Pennec, J. Gazalet, J. C. Kastelik, G. Lévêque, and B. Djafari-Rouhani, "Acousto-optic couplings in two-dimensional phoxonic crystal cavities," Appl. Phys. Lett. **101**(6), 061109 (2012).
41. T. R. Lin, C. H. Lin, and J. C. Hsu, "Enhanced acousto-optic interaction in two-dimensional phoxonic crystals with a line defect," J. Appl. Phys. **113**(5), 053508 (2013).
42. S. El-Jallal, M. Oudich, Y. Pennec, B. Djafari-Rouhani, V. Laude, J. C. Beugnot, A. Martínez, J. M. Escalante, and A. Makhoute, "Analysis of optomechanical coupling in two-dimensional square lattice phoxonic crystal slab cavities," Phys. Rev. B **88**(20), 205410 (2013).
43. S. El-Jallal, M. Oudich, Y. Pennec, B. Djafari-Rouhani, A. Makhoute, Q. Rolland, S. Dupont, and J. Gazalet, "Optomechanical interactions in two-dimensional Si and GaAs phoXonic cavities," J. Phys. : Condens. Matter **26**(1), 015005 (2014).
44. L. Kipfstuhl, F. Guldner, J. Riedrich-Möller, and C. Becher, "Modeling of optomechanical coupling in a phoxonic crystal cavity in diamond," Opt. Express **22**(10), 12410–12423 (2014).
45. M. Oudich, S. El-Jallal, Y. Pennec, B. Djafari-Rouhani, J. Gomis-Bresco, D. Navarro-Urrios, C. M. Sotomayor Torres, A. Martínez, and A. Makhoute, "Optomechanic interaction in a corrugated phoxonic nanobeam cavity," Phys. Rev. B **89**(24), 245122 (2014).
46. Y. Pennec, V. Laude, N. Papanikolaou, B. Djafari-Rouhani, M. Oudich, S. El-Jallal, J. C. Beugnot, J. M. Escalante, and A. Martínez, "Modeling light-sound interaction in nanoscale cavities and waveguides," Nanophotonics (posted 30 September 2014, in press).
47. M. Eichenfield, J. Chan, R. M. Camacho, K. J. Vahala, and O. Painter, "Optomechanical crystals," Nature **462**(7269), 78–82 (2009).
48. A. H. Safavi-Naeini, T. P. Mayer Alegre, J. Chan, M. Eichenfield, M. Winger, Q. Lin, J. T. Hill, D. E. Chang, and O. Painter, "Electromagnetically induced transparency and slow light with optomechanics," Nature **472**(7341), 69–73 (2011).
49. J. Chan, T. P. Mayer Alegre, A. H. Safavi-Naeini, J. T. Hill, A. Krause, S. Gröblacher, M. Aspelmeyer, and O. Painter, "Laser cooling of a nanomechanical oscillator into its quantum ground state," Nature **478**(7367), 89–92 (2011).
50. A. H. Safavi-Naeini, J. T. Hill, S. Meenehan, J. Chan, S. Gröblacher, and O. Painter, "Two-dimensional phononic-photonic band gap optomechanical crystal cavity," Phys. Rev. Lett. **112**(15), 153603 (2014).
51. O. Matsuda and O. B. Wright, "Reflection and transmission of light in multilayers perturbed by picosecond strain pulse propagation," J. Opt. Soc. Am. B **19**(12), 3028–3041 (2002).
52. E. Bormashenko, R. Pogreb, Z. Pogreb, and S. Sutovski, "Development of new near-infrared filters based on the sandwich polymer-chalcogenide glass-polymer composites," Opt. Eng. **40**(5), 661–662 (2001).
53. B. Temelkuran, S. D. Hart, G. Benoit, J. D. Joannopoulos, and Y. Fink, "Wavelength-scalable hollow optical fibres with large photonic bandgaps for CO_2 laser transmission," Nature **420**(6916), 650–653 (2002).
54. G. Benoit, S. D. Hart, B. Temelkuran, J. D. Joannopoulos, and Y. Fink, "Static and dynamic properties of optical microcavities in photonic bandgap yarns," Adv. Mater. **15**(24), 2053–2056 (2003).
55. Y. Ohmachi and N. Uchida, "Vitreous As_2Se_3; Investigation of acousto-optical properties and application to infrared modulator," J. Appl. Phys. **43**(4), 1709–1712 (1972).
56. M. E. Boyle and R. F. Cozzens, "Acousto-optic and linear electro-optic properties of organic polymeric materials," Naval Research Lab Washington DC, No. NRL-MR-6454 (1989).
57. S. Jakobs, A. Petrov, and M. Eich, "Suppression of stimulated Brillouin scattering in integrated chalcogenide waveguides," J. Opt. Soc. Am. B **31**(2), 178–188 (2014).
58. J. E. Mark, *Polymer Data Handbook* (Oxford University, 2009).
59. N. Stefanou, V. Yannopapas, and A. Modinos, "Heterostructures of photonic crystals: frequency bands and transmission coefficients," Comput. Phys. Commun. **113**(1), 49 (1998).
60. N. Stefanou, V. Yannopapas, and A. Modinos, "MULTEM2: A new version of the program for transmission and band-structure calculations of photonic crystals," Comput. Phys. Commun. **132**(1), 189 (2000).
61. R. Sainidou, N. Stefanou, I. E. Psarobas, and A. Modinos, "A layer-multiple-scattering method for phononic crystals and heterostructures of such," Comput. Phys. Commun. **166**(3), 197–240 (2005).
62. E. Almpanis, N. Papanikolaou, I. E. Psarobas, N. Stefanou, N. Glezos, B. Djafari-Rouhani, B. Bonello, V. Laude, and A. Martinez, "Acousto-optical engineering in polymeric multilayers," XXVII Panhellenic Conference on Solid State Physics and Materials Science, Limassol, Cyprus, 18-21 Sep. 2011, proceedings pp. 17–18.
63. K. Børkje, A. Nunnenkamp, J. D. Tenfel, and S. M. Girvin, "Signatures of nonlinear cavity optomechanics in the weak coupling regime," Phys. Rev. Lett. **111**(5), 053603 (2013).
64. C. Doolin, B. D. Hauer, P. H. Kim, A. J. R. MacDonald, H. Ramp, and J. P. Davis, "Nonlinear optomechanics in the stationary regime," Phys. Rev. A **89**(5), 053838 (2014).

#222544 - $15.00 USD Received 4 Sep 2014; revised 28 Oct 2014; accepted 2 Nov 2014; published 15 Dec 2014

1. Introduction

An acoustic wave in a material produces an internal strain field that induces periodic variations in the index of refraction through the photoelastic effect. These variations cause deflection and frequency shift of an incident light beam, effects which in the corpuscular picture can be viewed as absorption and emission processes of either a single (Bragg regime) or many (Raman-Nath regime) phonons by a photon [1]. A variety of interesting phenomena stemming from this, so-called acousto-optic (AO), interaction have lead to a plethora of diverse applications in photonic information processing, optical communication and laser technology.

From another point of view, the modulation induced by the acoustic wave is equivalent to a time-varying photonic crystal [2] which, however, can be described in the quasistatic approximation since the period of the acoustic field is much longer than that of the light wave [3–5]. Modulating appropriately designed photonic structures with bulk or surface acoustic waves provides further possibilities for tailoring the AO interaction and observing new and potentially useful effects [6–8].

In a typical AO device, an ultrasonic wave is usually launched into the material by a piezoelectric transducer. Alternatively, in ultrafast acoustics pump-probe experiments, picosecond laser pulses are used to generate and detect very short stress pulses, which correspond to coherent acoustic phonons, by monitoring in the time domain the changes they induce in the optical reflectivity of the sample surface [9–15]. On the other hand, inelastic light scattering by thermal phonons has also been proven to be an invaluable tool for probing vibrational properties of materials through Raman or Brillouin spectroscopy [16–18]. From the above studies it became clear that enhanced effects appear if localized or slow light modes are involved in the AO interaction.

It has been anticipated that appropriately engineered structures which exhibit dual spectral gaps, i.e., gaps for both photons and phonons, so-called phoxonic band-gap materials, can lead to applications that require better control of the AO interaction and, by all means, to impressive opportunities of manipulating light with acoustic waves [19]. So far, a variety of different phoxonic band-gap designs have been proposed and analyzed, including one-dimensional multilayer structures [20–23]; two-dimensional periodic arrays of air holes in a silicon, lithium niobate, or sapphire matrix [24–27] and two-dimensional crystals with veins [28]; periodic arrays of pillars deposited on a thin plate [29] and periodic arrays of holes in a silicon slab [30, 31]; three-dimensional crystals of metallic nanospheres in a dielectric host [32] and dielectric crystals with network topology [33]. The existence of phoxonic band gaps is the first step towards the realization of resonant cavities and slow-wave guiding structures [34–38], which confine simultaneously optical and acoustic waves in the same region of space for a long time period, thus enhancing their interaction [20–22, 39–46]. From a different point of view and indeed with a different perspective, the interplay between optical and acoustic waves is exploited in the emerging field of cavity optomechanics, where the radiation pressure of localized light in a cavity produces an elastic wave through mechanical deformation. In this context it has been shown that, in patterned silicon nanobeam structures, strong driven interactions are manifest between localized photons in the 1.5 μm telecommunication band and GHz-frequency phonons [47–49]. Two-dimensional optomechanical structures with dual resonant cavities have also been created and enhanced optomechanical coupling was demonstrated [50]. Most of the above studies refer to the weak-coupling limit, which is described by the linear AO interaction approximation, while some fingerprints of nonlinearity that have been observed defy a consistent interpretation. It is the purpose of the present paper to establish the limits of validity of this linear regime in a generic example of a one-dimensional phoxonic cavity and explain aspects of the underlying physics to a degree that goes beyond existing interpretation.

#222544 - $15.00 USD Received 4 Sep 2014; revised 28 Oct 2014; accepted 2 Nov 2014; published 15 Dec 2014

2. Theory

In the present work we shall be concerned with a stratified structure made of alternating layers of homogeneous and isotropic materials, grown along the z direction. A monochromatic compressional acoustic wave of angular frequency Ω, propagating perpendicular to the layers, induces an elastic displacement field $\hat{\mathbf{z}}u(z,t) = \hat{\mathbf{z}}\Re\mathrm{e}\left[u(z)\exp(-i\Omega t)\right]$ and changes the optical response of the structure, first through the displacement of the boundaries of each layer. This translates to a variation of the thickness of the j^{th} layer, which is characterized by a (relative) permittivity ε_j and permeability $\mu_j = 1$, given by $\delta d_j(t) = u(z_j,t) - u(z_{j-1},t)$, where z_j, z_{j-1} define the unperturbed positions of the layer boundaries. As a result, there is a dynamic change of the permittivity, throughout the structure, $\delta\varepsilon_{\mathrm{I}}(z,t)$, which equals $\varepsilon_j - \varepsilon_{j+1}$ for $u(z_j,t) > 0$ if $z_j < z < z_j + u(z_j,t)$, $\varepsilon_{j+1} - \varepsilon_j$ for $u(z_j,t) < 0$ if $z_j + u(z_j,t) < z < z_j$, and zero otherwise. In addition to this interface contribution, the bulk AO effect induces a modulation of the permittivity due to the spatial and temporal variation of the strain field, $S(z,t) = \partial_z u(z,t) = \Re\mathrm{e}\left[S(z)\exp(-i\Omega t)\right]$. If, as in our case, the layers are made of isotropic materials, this is given by [1]

$$\delta\overline{\overline{\varepsilon}}_{\mathrm{B}}(z,t) = -\varepsilon^2(z)S(z,t)\begin{pmatrix} p_{12}(z) & 0 & 0 \\ 0 & p_{12}(z) & 0 \\ 0 & 0 & p_{11}(z) \end{pmatrix}, \tag{1}$$

where $\varepsilon(z)$, $p_{12}(z)$ and $p_{11}(z)$ denote the relative permittivity and photoelastic coefficients of the material at point z. Therefore, the total perturbation of the permittivity of the structure that stems from the AO interaction consists of the above interface and bulk contributions

$$\delta\overline{\overline{\varepsilon}}(\mathbf{r},t) = \delta\varepsilon_{\mathrm{I}}(z,t) + \delta\overline{\overline{\varepsilon}}_{\mathrm{B}}(z,t). \tag{2}$$

In general, the electric field component of an EM wave propagating in an inhomogeneous medium characterized by a (relative) permittivity $\varepsilon(\mathbf{r})$ and permeability $\mu = 1$, subject to AO interaction described by a permittivity perturbation $\delta\overline{\overline{\varepsilon}}(\mathbf{r},t)$, satisfies the inhomogeneous differential equation

$$\sum_{\gamma}\Lambda_{\alpha\gamma}(\mathbf{r},t)E_{\gamma}(\mathbf{r},t) = \frac{1}{c^2}\sum_{\beta}\delta\varepsilon_{\alpha\beta}(\mathbf{r},t)\frac{\partial^2}{\partial t^2}E_{\beta}(\mathbf{r},t), \tag{3}$$

where

$$\Lambda_{\alpha\gamma}(\mathbf{r},t) = -[\nabla\times(\nabla\times)]_{\alpha\gamma} - \delta_{\alpha\gamma}\frac{\varepsilon(\mathbf{r})}{c^2}\frac{\partial^2}{\partial t^2}. \tag{4}$$

Equation (3) is derived from Maxwell equations if we ignore temporal variation of $\delta\overline{\overline{\varepsilon}}(\mathbf{r},t)$ compared to that of the EM field which is typically five orders of magnitude faster (quasistatic approximation). This equation can be solved using a Green's function technique. Introducing the (dyadic) Green's function through

$$\sum_{\gamma}\Lambda_{\alpha\gamma}(\mathbf{r},t)G^0_{\gamma\beta}(\mathbf{r},t;\mathbf{r}',t') = \delta_{\alpha\beta}\delta(\mathbf{r}-\mathbf{r}')\delta(t-t'), \tag{5}$$

we can write the solution of Eq. (3) in the form of a Born series

$$\begin{aligned}\mathbf{E}(\mathbf{r},t) = \mathbf{E}^0(\mathbf{r},t) &+ \frac{1}{c^2}\int d^3r'\int dt'\overline{\overline{G}}^0(\mathbf{r},t;\mathbf{r}',t')\delta\overline{\overline{\varepsilon}}(\mathbf{r}',t')\partial_{t'}^2\mathbf{E}^0(\mathbf{r}',t') \\ &+ \frac{1}{c^4}\int d^3r'\int dt'\int d^3r''\int dt''\overline{\overline{G}}^0(\mathbf{r},t;\mathbf{r}',t')\delta\overline{\overline{\varepsilon}}(\mathbf{r}',t')\end{aligned}$$

#222544 - $15.00 USD Received 4 Sep 2014; revised 28 Oct 2014; accepted 2 Nov 2014; published 15 Dec 2014

$$\times\partial_{t'}^2\overline{\overline{G}}^0(\mathbf{r}',t';\mathbf{r}'',t'')\delta\overline{\overline{\varepsilon}}(\mathbf{r}'',t'')\partial_{t''}^2\mathbf{E}^0(\mathbf{r}'',t'')+..., \tag{6}$$

where $\mathbf{E}^0$ is the solution of the corresponding homogeneous differential equation, i.e., the EM field in the absence of AO interaction. We again note that the time derivative of $\delta\overline{\overline{\varepsilon}}$ has been neglected, in the spirit of the quasistatic approximation. Assuming $\mathbf{E}^0$ to be a harmonic monochromatic wave of angular frequency ω, $\mathbf{E}^0(\mathbf{r},t)=\Re\mathrm{e}[\mathbf{E}^0(\mathbf{r})\exp(-i\omega t)]$, $\delta\overline{\overline{\varepsilon}}(\mathbf{r},t)=\Re\mathrm{e}[\delta\overline{\overline{\varepsilon}}(\mathbf{r})\exp(-i\Omega t)]$, and substituting into Eq. (6) the Fourier transform of the Green's dyadic, it can be shown that the electric field has the form

$$\mathbf{E}(\mathbf{r},t)=\Re\mathrm{e}\left[e^{-i\omega t}\sum_{n=0,\pm1,...}\mathbf{E}_n(\mathbf{r})e^{-in\Omega t}\right]. \tag{7}$$

This form implies that the total outgoing (transmitted+reflected) EM wave consists, in general, of an infinite number of monochromatic beams with angular frequencies $\omega,\omega\pm\Omega,\omega\pm2\Omega,...$, which are produced by elastic and inelastic photon scattering that involves absorption and/or emission of zero, one, two,... phonons.

The above result can be understood as follows. Because of the relatively slow periodic variation of the optical response of the system due to the AO interaction, one can introduce time-dependent amplitudes for the scattered EM field at given angular frequency ω. These amplitudes are practically constant over the short period of the EM wave and lead to a time-dependent periodic complex reflection coefficient

$$r(t)=r(t+2\pi/\Omega)=\sum_{n=0,\pm1,...}r_ne^{-in\Omega t} \tag{8}$$

and a similar Fourier expansion for the transmission coefficient. Consequently, for a monochromatic incident EM wave of angular frequency ω, the reflected and transmitted fields consist of an infinite number of beams with angular frequencies $\omega+n\Omega$, $n=0,\pm1,\pm2,...$, as we deduced in Eq. (7). The corresponding reflectivity, averaged over a time period of the acoustic wave, is

$$<\mathscr{R}(t)>=<r(t)r^*(t)>=\frac{\Omega}{2\pi}\sum_{n,n'}r_nr_{n'}\int_0^{2\pi/\Omega}e^{-i(n-n')\Omega t}dt=\sum_n|r_n|^2, \tag{9}$$

which defines the elastic (Rayleigh) and inelastic reflected intensities, $\mathscr{R}_n\equiv|r_n|^2$, for $n=0$ and $n\neq0$, respectively.

If we restrict ourselves to first order in the expansion of Eq. (6), a simple analytical treatment is possible. Since the structure under study is invariant in the $x-y$ plane, if we consider normally incident monochromatic light of angular frequency ω, linearly polarized along the x-axis, we have $\mathbf{E}^0(\mathbf{r},t)=\hat{\mathbf{x}}\Re\mathrm{e}\left[E^0(z)\exp(-i\omega t)\right]$ and, following Matsuda and Wright [51], we obtain to first order Born approximation, denoted by a superscript (1), the following analytical expression for the reflection amplitude associated with the one-phonon-absorption (anti-Stokes) process

$$r_1^{(1)}=\frac{i\omega}{4cn_\mathrm{h}}\left[\int dzp_{12}(z)\varepsilon^2(z)\frac{\partial u(z)}{\partial z}\{E^0(z)/E_\mathrm{in}\}^2+\sum_j(\varepsilon_{j+1}-\varepsilon_j)u(z_j)\{E^0(z_j)/E_\mathrm{in}\}^2\right], \tag{10}$$

where E_in is the input electric field level and n_h is the refractive index of the embedding host medium. A similar expression holds for the corresponding Stokes amplitude $r_{-1}^{(1)}$ with u^* instead of u. This first order Born approximation, which is referred to as linear photoelastic model, is widely used in explaining pump-probe and Brillouin light scattering experiments.

#222544 - $15.00 USD Received 4 Sep 2014; revised 28 Oct 2014; accepted 2 Nov 2014; published 15 Dec 2014

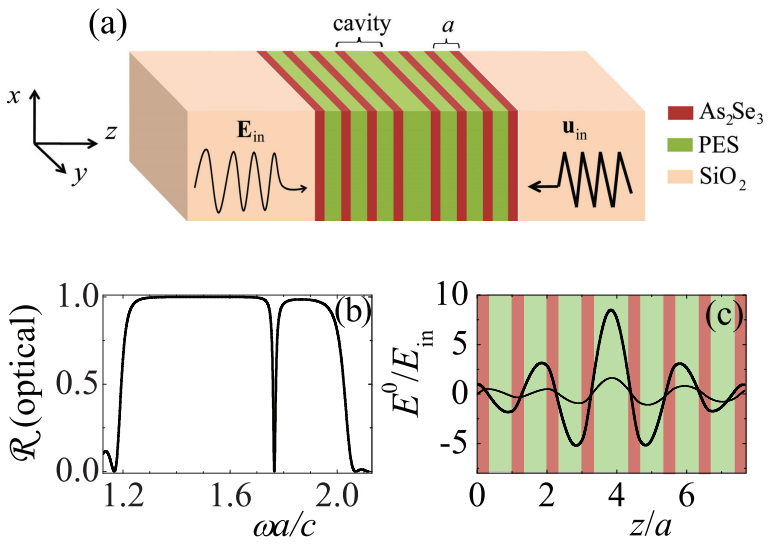

Fig. 1. (a) Schematic view of the one-dimensional As_2Se_3/PES multilayer structure under consideration. (b) Associated optical reflectivity spectrum at normal incidence, without acoustic excitation. (c) Corresponding electric field amplitude profile, normalized to the input field level E_{in}, at the resonance frequency $\omega_0 a/c = 1.775$ (thick line: Real part, thin line: Imaginary part).

3. Results and discussion

We consider a stack of alternating arsenic triselenide glass (As_2Se_3) and polyethersulphone (PES) layers, which form a simultaneously optical and acoustic cavity between two Bragg mirrors, embedded in a silica (SiO_2) matrix. Such As_2Se_3/PES multilayers can be thermally co-drawn into precisely layered structures and exhibit ultra-low optical losses [52–54]. The Bragg mirrors consist of three periods, with lattice constant a, of $As_2Se_3(a/3)$/PES$(2a/3)$ bilayers (the respective layer thickness is given in parenthesis) and the cavity in the middle is an $As_2Se_3(a/3)$/PES(a)/$As_2Se_3(a/3)$ trilayer, as shown in Fig. 1(a). The relevant material properties for As_2Se_3, PES, SiO_2 are determined by the index of refraction n=2.83, 1.55, and 1.44; photoelastic coefficient p_{12} =0.27, 0.30, and 0.27; mass density ρ= 4.64, 1.37, and 2.20 g/cm^3; longitudinal sound velocity c_l = 2250, 2260, and 5965 m/s, respectively [55–58].

Figure 1(b) displays the optical reflectivity spectrum of the multilayer stack under consideration without acoustic excitation, at normal incidence, calculated by the electrodynamic layer-multiple-scattering method [59, 60]. The occurrence of a cavity mode is manifested as a sharp dip in the reflection spectrum at $\omega_0 a/c = 1.775$ within the first EM Bragg gap of the periodic stack. This mode has a Q factor of about 150 and the associated field distribution is strongly localized in the cavity region as shown in Fig. 1(c).

Corresponding calculations by the elastodynamic layer-multiple-scattering method [61] reveal the existence of acoustic cavity resonant modes in the same structure, which are also manifested as sharp dips in the reflectivity spectrum for a normally incident compressional acoustic wave, as shown in Fig. 2(a). The lower mode at $\Omega_1 a/c_{l;\text{SiO}_2} = 1.25$, within the first acoustic Bragg gap of the periodic stack, has a Q factor of about 1200 and the associated displacement field is symmetric upon reflection with respect to the center of the cavity, which implies that the corresponding strain field distribution is antisymmetric, as shown in Figs. 2(b) and 2(c). The higher resonant mode $\Omega_2 a/c_{l;\text{SiO}_2} = 2.31$ within the second acoustic Bragg gap of the periodic

#222544 - $15.00 USD Received 4 Sep 2014; revised 28 Oct 2014; accepted 2 Nov 2014; published 15 Dec 2014

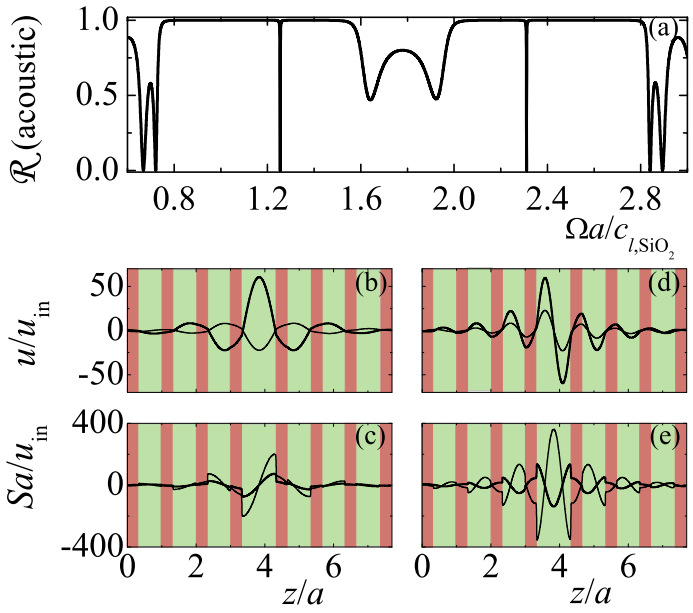

Fig. 2. (a) Acoustic reflectivity spectrum of the structure of Fig. 1(a) for a normally incident compressional acoustic wave. Displacement and strain field amplitude profiles in the multilayer stack, normalized to to the input displacement level u_{in}, associated with the lower (at $\Omega_1 a/c_{l;\mathrm{SiO_2}} = 1.25$) and higher (at $\Omega_2 a/c_{l;\mathrm{SiO_2}} = 2.31$) resonant modes are depicted in diagrams (b), (c) and (d), (e) respectively. Real and imaginary parts of the fields are shown by thick and thin lines, respectively. Color stripes in the background of the field distribution diagrams depict the regions of As_2Se_3 and PES [see Fig. 1(a)].

stack, has a Q factor of about 2200 and the associated displacement (strain) field is antisymmetric (symmetric) upon reflection with respect to the center of the cavity, as shown in Figs. 2(d) and 2(e). Of course, the Q factors of the optical and acoustic cavity modes can be made arbitrarily high by increasing the width of the Bragg mirrors, provided that dissipative losses are neglected. It is worth noting that, here, we chose to represent the EM and acoustic spectral ranges using an appropriate dimensionless frequency, $\omega a/c$ and $\Omega a/c_{l;\mathrm{SiO_2}}$, respectively, so that the results remain valid at any frequency region provided that the thickness of the layers is scaled accordingly. For example, choosing $a = 440$ nm, the optical resonance is tuned at a wavelength $\lambda_0 = 1557$ nm while the acoustic resonances appear at frequencies $f_1 = 2.7$ GHz and $f_2 = 5$ GHz. Though, in this case, optical absorption in the constituent materials is small, ultrasonic losses cannot be neglected and may be taken into account by assuming complex propagation velocities with an imaginary part by 2-3 orders of magnitude smaller than their real part [21]. These losses reduce the Q factor of the corresponding cavity modes but do not alter qualitatively our results; therefore, for simplicity, we shall not consider them here.

We now assume an EM wave at the optical resonance frequency, $\omega_0 a/c = 1.775$, incident normally on the given structure under continuous excitation by a compressional acoustic wave at the resonance frequency $\Omega_2 a/c_{l;\mathrm{SiO_2}} = 2.31$, normally incident from the opposite side as shown in Fig. 1(a). The continuous variation of the permittivity function implied by Eq. (2) is taken into account through a discretization approach by subdividing each layer into a large number of homogeneous elementary sublayers, at each time step. In all cases examined here, about 500 sublayers in the whole structure and 50 time steps within the period of the acoustic wave

#222544 - $15.00 USD Received 4 Sep 2014; revised 28 Oct 2014; accepted 2 Nov 2014; published 15 Dec 2014

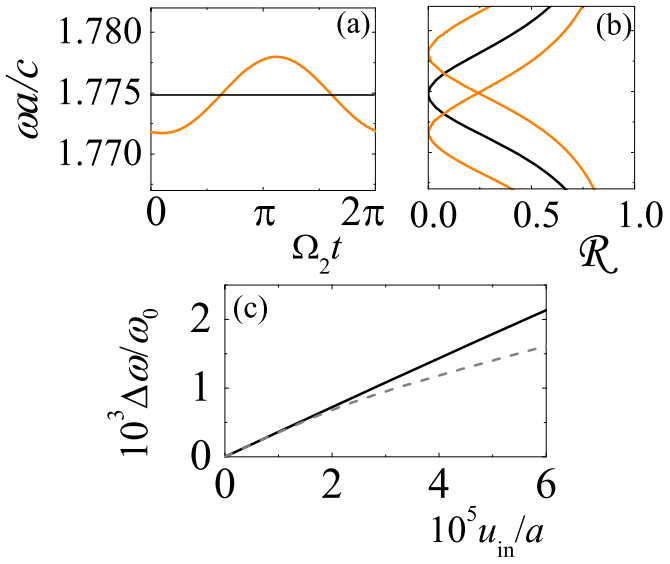

Fig. 3. (a) Oscillatory behavior of the optical resonance frequency [see Fig. 1(b)] under continuous excitation by a normally incident compressional acoustic wave [see Fig. 1(a)] at the resonance frequency $\Omega_2 a/c_{l;\mathrm{SiO_2}} = 2.31$. The straight horizontal line shows the unperturbed optical resonance frequency, ω_0. (b) Snapshots of the optical reflectivity at normal incidence, at which maximum frequency shift of the resonance, $\Delta\omega$, is obtained. The input displacement level in (a) and (b) is $u_{\mathrm{in}}/a = 5\times10^{-5}$. (c) Maximum frequency shift of the optical resonance as a function of the input acoustic displacement level. Solid line: Full treatment. Dashed line: First-order Born approximation.

suffice to obtain excellent convergence. When the acoustic excitation is switched on, the optical reflectivity spectrum varies periodically in time with the period of the acoustic wave about its unperturbed position in the absence of AO interaction. Indeed, to first-order approximation,

$$\begin{aligned}\mathscr{R}(\omega,t) &= |r_0^{(0)}(\omega)+r_1^{(1)}(\omega)\exp(-i\Omega t)+r_{-1}^{(1)}(\omega)\exp(i\Omega t)|^2 \\ &\cong |r_0^{(0)}(\omega)|^2+2\Re\mathrm{e}[r_0^{(0)*}(\omega)\{r_1^{(1)}(\omega)\exp(-i\Omega t)+r_{-1}^{(1)}(\omega)\exp(i\Omega t)\}] \quad (11)\end{aligned}$$

and $<\mathscr{R}(\omega,t)>=|r_0^{(0)}(\omega)|^2$. Let us assume an input displacement amplitude $u_{\mathrm{in}} = 5\times10^{-5}a$, which corresponds to an input strain level of about 10^{-4}, that is an order of magnitude lower than that considered in [20]. We note that, for $a = 440$ nm, $u_{\mathrm{in}} = 0.022$ nm, which is experimentally achievable [12]. On the other hand, inside the cavity the strain level does not exceed 2%, which can be supported by mechanically flexible polymer materials such as PES [58]. Even though the overall spectral features and the position of the optical gap do not change much as time evolves, the position of the optical cavity mode oscillates in time with the period of the acoustic wave as expected and, if the acoustic excitation is at resonance, the amplitude of this oscillation, $\Delta\omega$, is relatively large as shown in Figs. 3(a) and 3(b). It is worth noting that the major contribution in our case comes from the bulk AO effect ($\sim 60\%$), while the interface AO contribution is smaller ($\sim 40\%$). The modulation of the optical cavity mode by the acoustic wave can be understood as follows. Assuming that the mechanical vibrations do not affect drastically the structure under consideration so that both photonic band gap and cavity mode are maintained, the induced periodic variation in the permittivity and thickness of the

#222544 - $15.00 USD Received 4 Sep 2014; revised 28 Oct 2014; accepted 2 Nov 2014; published 15 Dec 2014

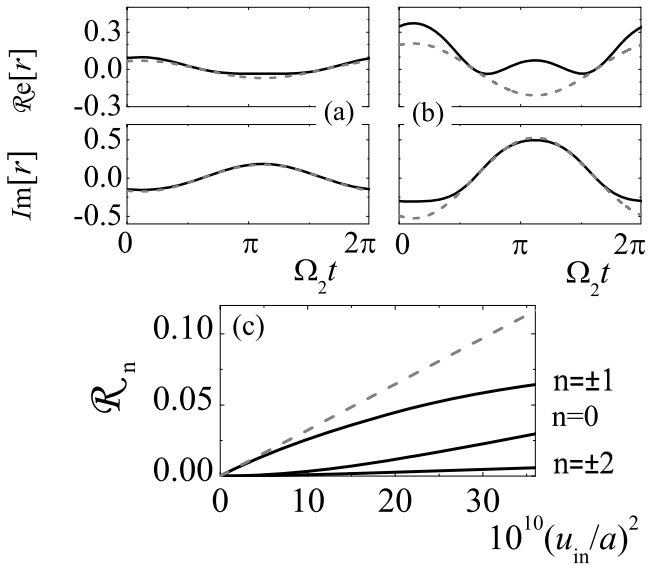

Fig. 4. Time variation of the optical reflection coefficient at the eigenfrequency of the cavity $\omega_0 a/c = 1.775$ [see Fig. 1(b)] under the action of a normally incident compressional acoustic wave at the resonance frequency $\Omega_2 a/c_{l;\mathrm{SiO_2}} = 2.31$ [see Fig. 2(a)] for $u_{\mathrm{in}}/a = 2\times10^{-5}$(a) and $u_{\mathrm{in}}/a = 5\times10^{-5}$(b). (c) Corresponding intensities of the elastically and inelastically reflected light beams as a function of the input acoustic intensity factor $(u_{\mathrm{in}}/a)^2$. The difference between Stokes and anti-Stokes components is not discernible in the scale of the figure. The dashed lines in the diagrams show the results of the first-order Born approximation given by Eq. (10).

cavity results in a periodic oscillation of the position of the optical cavity mode in the gap with the same period. If the strain distribution, associated with the acoustic cavity mode involved is symmetric as in the present case under consideration, the corresponding photon-phonon interaction is enhanced because of the simultaneous concentration of the respective fields in the cavity region and nonvanishing by symmetry first-order coupling element. In the wave picture this strong interaction is manifested as a relatively large-amplitude oscillation of the position of the optical resonance. Correspondingly, in the corpuscular picture, one expects strong inelastic light scattering with considerable probabilities for absorption and emission of many phonons by a photon. For relatively low levels of input displacement ($u_{\mathrm{in}}/a < 2\times10^{-5}$), the exact calculation is in good agreement with the first-order Born approximation and $\Delta\omega$ varies linearly with u_{in}, which is not the case for larger values of u_{in} where the results of the first-order Born approximation yield a trend to saturation and deviate from the linear $\Delta\omega$ versus u_{in} behavior as shown in Fig. 3(c). This can be understood if we bear in mind that the first-order Born approximation corresponds to single-phonon exchange processes and refers to the weak-coupling limit that requires the dwell time of a photon in the cavity to be shorter than the time necessary to absorb a second phonon or, equivalently, the coupling rate, quantified by $\Delta\omega$, not to exceed the optical cavity linewidth. Indeed, an increased $\Delta\omega$ would imply stronger variations of the complex reflection coefficient at ω_0, and thus higher-order inelastic scattering, beyond the linear regime, as we shall discuss here below.

In Fig. 4(a) we depict the calculated time variation of the optical complex reflection coefficient at the resonance frequency $\omega_0 a/c = 1.775$ [see Fig. 1(b)] under the action of a continuous

#222544 - $15.00 USD Received 4 Sep 2014; revised 28 Oct 2014; accepted 2 Nov 2014; published 15 Dec 2014

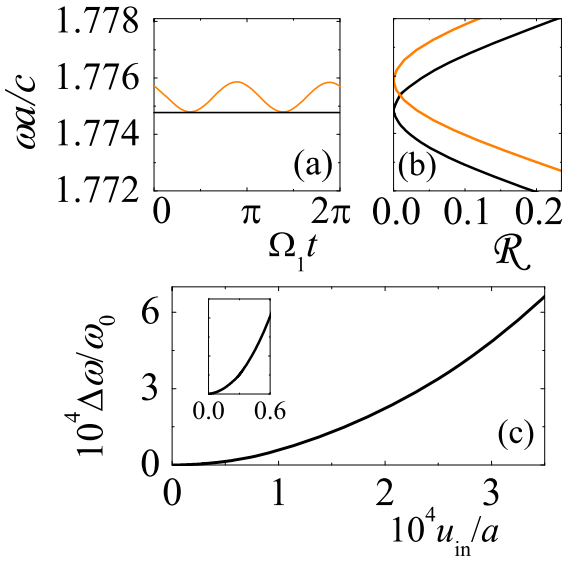

Fig. 5. (a) Oscillatory behavior of the optical resonance frequency [see Fig. 1(b)] under continuous excitation by a normally incident compressional acoustic wave [see Fig. 1(a)] at the resonance frequency $\Omega_1 a/c_{l;\mathrm{SiO_2}} = 1.25$. The straight horizontal line shows the unperturbed optical resonance frequency, ω_0. (b) Snapshots of the optical reflectivity at normal incidence, at which maximum frequency shift of the resonance, $\Delta\omega$, is obtained. The input displacement level in (a) and (b) is $u_{\mathrm{in}}/a = 3\times10^{-4}$. (c) Maximum frequency shift of the optical resonance as a function of the input acoustic displacement level. A detail view demonstrating the quadratic behavior at low u_{in} is shown in the inset.

normally incident compressional acoustic wave at the resonance frequency $\Omega_2 a/c_{l;\mathrm{SiO_2}} = 2.31$ [see Fig. 2(a)] with a relatively low input displacement level $u_{\mathrm{in}}/a = 2\times10^{-5}$. The results of the exact treatment exhibit a smooth sinusoidal-like variation, in good agreement with the first-order Born approximation. The corresponding Fourier spectrum is essentially dominated by the first-order contribution while all higher-order terms are negligibly small, as shown in Fig. 4(c). However, as the input displacement level increases, strong interaction takes place. The scattering process is no longer linear on the AO coupling parameter and many terms must be taken into account in the Born-series expansion of Eq. (6). In the corpuscular picture, this implies strong probability amplitudes for multiphonon absorption and emission processes. Figure 4(b) displays results corresponding to those shown in Fig. 4(a) for a relatively high input displacement level $u_{\mathrm{in}}/a = 5\times10^{-5}$. In this case, we no longer obtain a simple sinusoidal-like variation and the first-order Born approximation fails to reproduce the exact time variation of the optical complex reflection coefficient. This is also reflected in the corresponding Fourier spectrum where, in addition to the first harmonics ($n = \pm1$), there are also non-negligible second-order Stokes and anti-Stokes components as well as an elastic-scattering component. The latter is ascribed to multiphonon processes with simultaneous absorption and emission of the same number of phonons because the reflectivity at the optical resonance vanishes in the unperturbed static structure and thus the reflection coefficient that we consider is entirely modulated by the AO interaction. The linear variation of $\mathscr{R}_{\pm1}$ versus u_{in}^2 observed in Fig. 4(c) in the first-order Born approximation, as expected on the basis of Eq. (10), can be explained as follows. In this approximation, a single phonon is absorbed (or emitted) by one photon, which describes a lin-

#222544 - $15.00 USD Received 4 Sep 2014; revised 28 Oct 2014; accepted 2 Nov 2014; published 15 Dec 2014

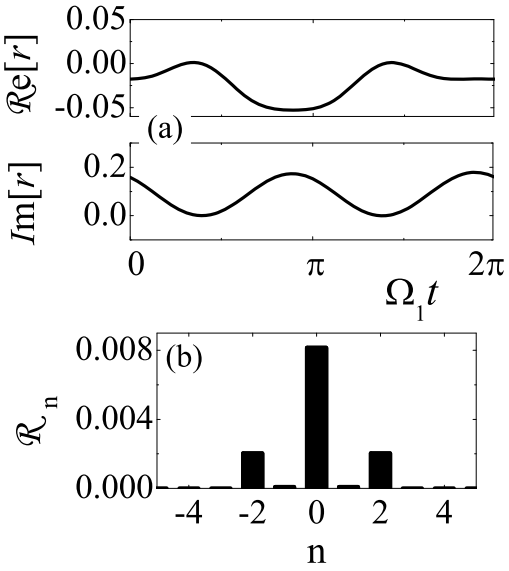

Fig. 6. (a) Time variation of the optical reflection coefficient at the eigenfrequency of the cavity $\omega_0 a/c = 1.775$ [see Fig. 1(b)] under the action of a normally incident compressional acoustic wave at the resonance frequency $\Omega_1 a/c_{l;\mathrm{SiO_2}} = 1.25$ [see Fig. 2(a)] with input displacement level $u_{\mathrm{in}}/a = 3\times 10^{-4}$. (b) Corresponding intensities of the elastically and inelastically reflected light beams for the given input displacement.

ear regime [dashed line in Fig. 4(c)]: The intensity of the inelastically reflected light beam is proportional to the number of the absorbed (or emitted) phonons, i.e., to the intensity of the acoustic wave that is proportional to u_{in}^2. On the contrary, beyond the first-order Born approximation where a given number of phonons can be exchanged in many different ways by the photons, the intensity of the first-order inelastically reflected light beam is reduced, as can be actually observed in Fig. 4(c). It is also worth-noting that there is a small difference between the intensities of the Stokes and anti-Stokes inelastically reflected beams, $\mathscr{R}_n \neq \mathscr{R}_{-n}$, which is, however, not discernible in the scale of Fig. 4(c). This difference can be understood from the fact that an acoustic resonant mode does not strictly correspond to a standing wave and, therefore, the time-reversed process requires, also, inversion of the direction of propagation of the acoustic wave. Indeed, in the absence of absorptive losses, the Stokes components of the reflectivity are identical to their anti-Stokes counterparts if we reverse the propagation direction of the acoustic wave, and vice versa. However, in the presence of dissipation, this correspondence is no longer valid because time-reversal symmetry is broken.

We now consider the acoustic excitation tuned at the lower resonance frequency $\Omega_1 a/c_{l;\mathrm{SiO_2}} = 1.25$ [see Fig. 2(a)] where, contrary to the previous case, the corresponding displacement and strain field patterns are symmetric and antisymmetric upon reflection with respect to the cavity center, as shown in Figs. 2(b) and 2(c), respectively. Therefore, both bulk and interface terms of the reflection amplitudes in the first-order Born approximation should vanish identically according to Eq. (10) and this holds for all odd-order contributions [62]. However, since we consider a finite structure, we have resonant modes that are excited by an externally incident wave and not true bound states. Therefore, the associated field patterns have only approximately a given parity and consequently there is a small residual first-order as well as higher odd-order contributions to the AO interaction. In this case, to leading order we have

#222544 - $15.00 USD Received 4 Sep 2014; revised 28 Oct 2014; accepted 2 Nov 2014; published 15 Dec 2014

$$\mathscr{R}(\omega,t) = |r_0^{(0)}(\omega) + r_0^{(2)}(\omega) + r_2^{(2)}(\omega)\exp(-2i\Omega t) + r_{-2}^{(2)}(\omega)\exp(2i\Omega t)|^2 \cong$$
$$|r_0^{(0)}(\omega)|^2 + 2\Re\mathrm{e}[r_0^{(0)*}(\omega)\{r_0^{(2)}(\omega) + r_2^{(2)}(\omega)\exp(-2i\Omega t) + r_{-2}^{(2)}(\omega)\exp(2i\Omega t)\}], \quad (12)$$

which describes an optical reflectivity spectrum that varies periodically in time with half the period of the acoustic wave about its unperturbed position, $|r_0^{(0)}(\omega)|^2$, shifted roughly by $2\Re\mathrm{e}[(r_0^{(0)*}(\omega)r_0^{(2)}(\omega)]$ which is of the order of the oscillation amplitude. This behavior is indeed observed in Figs. 5(a) and 5(b) while Fig. 5(c) displays a characteristic quadratic increase of $\Delta\omega$ versus u_{in} that is consistent with the leading order of the AO coupling. Correspondingly, the Fourier spectrum of the time-dependent optical reflection coefficient at the resonance frequency $\omega_0 a/c = 1.775$ is also dominated by the two-phonon exchange Stokes, anti-Stokes, and Rayleigh contributions as shown in Fig. 6. Such features of the AO interaction when first-order coupling vanishes by symmetry have also been noticed by others in different phoxonic structures [14, 40, 42, 43, 45]. In this respect, our simple one-dimensional model phoxonic cavity allows us to provide a consistent interpretation of this generic behavior, enabling physical insight, which is also useful in connection with the field of cavity optomechanics. If the optomechanical coupling factor, obtained in the framework of first-order perturbation theory where only single-phonon exchange processes are involved, vanishes identically, the description of the interaction between optical and mechanical degrees of freedom needs to be properly generalized [63, 64].

4. Conclusion

In summary, we reported a thorough study of different aspects relating to the occurrence of nonlinear AO effects in a one-dimensional polymer/glass multilayer phoxonic cavity, by means of rigorous full electro-elastodynamic simulations together with linear photoelastic model calculations and discussed the limits of validity of the latter. Our results provide evidence that the linear-response regime breaks down when either the pump acoustic excitation increases or the first-order AO interaction coupling element vanishes by symmetry, revealing the manifestation of multiphonon exchange effects by a photon, such as new generic features in the variation of the optical frequency shift that determines the optomechanical coupling factor as well as in the inelastic and elastic light scattering intensities. These effects stem from higher-order multiple-scattering contributions and not from intrinsic nonlinearities of the constituent materials, which can be relatively weak. Phoxonic architectures, such as those studied in the present work, provide an efficient and versatile platform for tailoring the AO interaction and controling photons with phonons. The strong optomechanical coupling that can be achieved in phoxonic cavities makes them suitable for a variety of applications, including stimulated phonon emission through cavity parametric instability [14].

Acknowledgment

This work was co-funded by the European Union (ESF) and the Greek state under the ARISTEIA II action (project THUNDER) of the operational program "Education and lifelong learning".